



## Structure of a freely propagating rich CH<sub>4</sub>/air flame containing triphenylphosphine oxide and hexabromocyclododecane

A.G. Shmakov<sup>a</sup>, V.M. Shvartsberg<sup>a</sup>, O.P. Korobeinichev<sup>a,\*</sup>, M.W. Beach<sup>b</sup>,  
T.I. Hu<sup>b</sup>, T.A. Morgan<sup>b</sup>

<sup>a</sup> Institute of Chemical Kinetics and Combustion, Novosibirsk, 630090 Russia

<sup>b</sup> The Dow Chemical Company, Midland, MI 48667, USA

Received 15 May 2006; received in revised form 22 February 2007; accepted 1 March 2007

Available online 18 April 2007

### Abstract

The chemical and thermal structure of a premixed rich CH<sub>4</sub>/air/N<sub>2</sub> flame ( $\phi = 1.18 \pm 0.02$ ) that contains either triphenylphosphine oxide [(C<sub>6</sub>H<sub>5</sub>)<sub>3</sub>PO] or hexabromocyclododecane [C<sub>12</sub>H<sub>18</sub>Br<sub>6</sub>] and that is stabilized on a Mache–Hebra burner was studied experimentally using molecular beam mass spectrometry (MBMS) and the microthermocouple technique. Compounds such as hexabromocyclododecane (HBCD) and triphenylphosphine oxide (TPPO) are representative flame-retardant additives that are added to polymers to reduce the flammability of the base polymer. Both compounds provide flame retardation in the gas phase by the production of active species that effectively scavenge key combustion radicals to shut down the combustion process. The MBMS method was used to determine the concentration profiles of stable and active species directly in the flame, which includes atoms as well as free radicals. Thin thermocouples were employed to determine temperature profiles in a flame stabilized on a Mache–Hebra burner at a pressure of 1 atm. A comparison of the experimental data and simulation results for the flame structure shows that MBMS is suitable for studying the structure of flames that are close to freely propagating conditions. The relative effectiveness of flame inhibition by the compounds tested was estimated from changes in the peak concentrations of H and OH radicals in the flame and from changes in the estimated flame velocity.

© 2007 The Combustion Institute. Published by Elsevier Inc. All rights reserved.

**Keywords:** Flame inhibition; Burning velocity; Polymer retardants; Flame structure

### 1. Introduction

Polymeric materials offer many advantages and are used in many commercial applications. To meet the regulatory requirements for low flammability in many commercial applications, flame-retardant additives are blended with many organic polymers to lower the overall flammability and improve the poly-

\* Corresponding author. Fax: +7 383 3307350.

E-mail address: [korobein@kinetics.nsc.ru](mailto:korobein@kinetics.nsc.ru)  
(O.P. Korobeinichev).

mer's fire performance. These additives reduce the base polymer flammability via their reactive nature, which is usually activated prior to and/or during the degradation of base polymer. The mechanisms underlying the effects of such retardants can be very different. Flame retardants can promote a condensed-phase mechanism whereby a film or char layer is formed that isolates the remaining bulk polymer from the fire—usually an impermeable layer is formed that prevents degraded polymer (fuel) from reaching the fire. Flame-retardant additives can also proceed via a gas-phase mechanism where the flame retardant degrades to form volatile gas-phase species. These gas-phase species can act via several pathways, but many promote some sort of chemical inhibition of flame reactions. To more effectively use well-known flame retardants and to aid in the design of new candidates, it is important to understand their fundamental mechanism and effectiveness of action.

Much of the previous work on mechanistic studies of flame-retardant activity has focused on the thermal degradation of the flame retardant via traditional thermal analysis, evolved-gas, and various analytical pyrolysis methods [1–4]. These methods are limited to the detection of relatively stable degradation species and are unsuitable for detection of unstable radicals and other species that are key components of a complete understanding of the active flame-retardant mechanism. Previous work on the direct detection of flame-retardant species in flames was limited to detection and depletion of OH radicals by laser-induced fluorescence (LIF) [5].

Detailed studies of the chemical structure of flames with retardants by molecular beam mass spectrometry (MBMS) should help understand the fundamental gas-phase interactions involved with flame retardants. In particular, MBMS will allow confirmation of whether the flame-retardant mechanism involves the inhibition of chain reactions by chain termination or a thermal effect. Inhibition of chain reactions could originate from the flame retardant itself or a degradation species formed from the flame retardant. MBMS should allow confirmation of the active species in a possible chain-termination reaction, as well as the direct analysis of key combustion species such as OH and H. In particular, direct detection of the reduction of OH and H levels after addition of a retardant should correspond to the fundamental effectiveness of the retardant.

For this work, the thermal and chemical structure of a  $\text{CH}_4/\text{air}/\text{N}_2$  flame was studied under near-freely-propagating conditions after addition of flame retardants. MBMS was used to measure the concentrations of atoms and radicals directly in the flame. The selection of a flame in close to freely propagating conditions provides a more accurate analysis of

key species in the flame. The absence of heat losses in such a flame, unlike a flame stabilized on a flat burner, considerably simplifies comparison of experimental and simulation results for the flame structure. In addition, our studies have shown that in the case of a flame under near-freely-propagating conditions, the perturbation introduced by the probe is much smaller because of the higher flow velocity of the flame. The absence of a perforated (or porous) disk, which is typically used in a flat-burner flame configuration, simplifies the procedure of adding solid or low-volatile retardants to the gas flow and reduces their respective losses.

At present, experimental data on the structure of flames under nearly adiabatic conditions obtained by MBMS are not available in the literature. Hastie and Bonnell [6] performed only a qualitative MBMS study of the structure of  $\text{H}_2/\text{O}_2/\text{N}_2$  and  $\text{CH}_4/\text{O}_2/\text{N}_2$  flames stabilized on a Bunsen burner at atmospheric pressure. This work involved the addition of  $\text{CF}_3\text{Br}$  or trimethylphosphate  $(\text{CH}_3\text{O})_3\text{PO}$  and did not involve calibrations, so absolute concentrations of flame species were not determined. As a rule, at atmospheric pressure, flames have a narrow combustion zone (about 1 mm) and a high temperature of the final combustion products. In previous works, the mechanism of inhibition and extinction of hydrocarbon flames by organophosphorus compounds was studied [7–11]. It was shown that these inhibitors and/or their decomposition products catalyze recombination reactions of H and OH in flame front. These previous studies were limited to only liquids and relatively volatile organophosphorus inhibitors. The present work focuses on the effect of solid commercially available flame retardants, hexabromocyclododecane (HBCD) and triphenylphosphine oxide (TPPO), on flames. The MBMS technique is used to study the chemical structure of flames under near-adiabatic conditions after addition of these flame retardants. The potential for estimating the flame-retardant effectiveness from its impact on the concentration of H and OH radicals in flame is examined.

## 2. Experimental technique

We studied the structure of a premixed  $\text{CH}_4/\text{air}/\text{N}_2$  (9.18/74.2/16.62) flame with and without flame retardants stabilized on a Mache–Hebra burner at atmospheric pressure. The initial temperature of the combustible mixture was 368 K. The composition of the combustible mixture was chosen so that the final flame temperature was not higher than 1700 °C and the equivalence ratio  $\phi$  was  $1.18 \pm 0.02$ . The choice of a flame with this final temperature was motivated

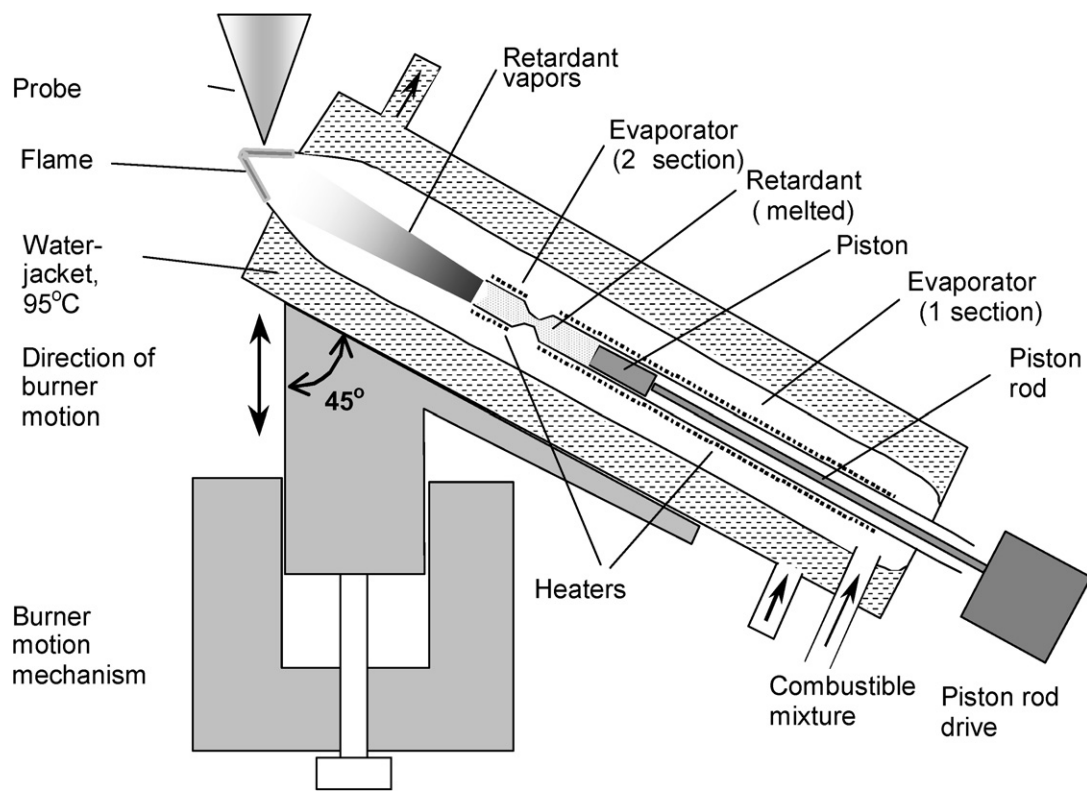


Fig. 1. Scheme of experimental setup.

by the possibility of using a quartz probe for sampling from the flame.

The burner used a quartz tube 27 cm long, tapered at one end (a factor of 4.7 decrease in the cross-sectional area over a length of 3 cm), and a nozzle exit diameter of 1 cm. The burner was fitted with a temperature-controlled jacket coupled to a thermostat. The burner was tapered to achieve a uniform cross-sectional distribution of the flow velocity at the tube end and a regular flame cone (a so-called Mache–Hebra burner [12]). To simplify the measurements, the burner axis was tilted at  $\approx 45^\circ$  from the vertical. This allowed concentration profile measurements in the direction perpendicular to the flame front. Fig. 1 shows the experimental setup.

The concentration of the flame retardants—triphenylphosphine oxide ( $(C_6H_5)_3PO$ , TPPO,  $T_{melt} = 153^\circ C$ ,  $T_b = 350^\circ C$ ) and hexabromocyclododecane ( $C_{12}H_{18}Br_6$ , HBCD,  $T_{melt} = 153^\circ C$ , decomposition at  $T > 260^\circ C$ )—in the combustible mixture was such that the flame velocity decreased only slightly (by a factor of 1.2–1.8). The concentration of the retardants was varied by changing the rate of supply of their vapor to the flow of the combustible mixture. This was done using a special evaporator placed inside the burner. The evaporator was a quartz tube, which had

an inner diameter of 3.6 mm and consisted of two sections (Fig. 1). Each of the sections was furnished with a heater and a thermocouple for temperature control. A Teflon piston was placed inside the tube and driven by a step motor. The latter was outside the burner. The retardant tested was placed in the tube (section 1) and heated to the melting point. The melt was supplied by the piston to the end of the tube (section 2), where the temperature was high enough to vaporize the retardant. For TPPO and HBCD, the temperature of section 2 was 300 and  $220^\circ C$ , respectively. The distance from the evaporator to the burner nozzle exit was chosen to ensure uniform mixing of the vapor or decomposition products of the additive in the combustible mixture flow, as well as to minimize any deposition on the inner walls of the burner. The losses of additive inside the burner were estimated at about 4–16% of the original mass introduced into the combustible-mixture flow. The mass of evaporated retardants was determined based on the mass difference before and after each experiment. After an experiment, any deposited retardant on the inner walls of the burner was washed off with solvent. The mass of deposited retardant was determined after removal of solvent and subsequent weighing. Thus, amount of dopant loaded into the flame was calculated based on the speed of

feeding of the melted retardant, the amount of losses of deposited retardant, and the flow of the combustible mixture. This procedure was repeated after each experiment.

The height of the flame cone was about 10 mm and was varied by changing the flow rate of the combustible mixture. The height of the flame cone was measured from its top up to the center of the basis (center of a circle) along an axis of symmetry. For each experiment, the flow rate of the combustible mixture for the flame without additives was about  $36 \text{ cm}^3/\text{s}$ . The addition of the retardants to the flame decreased the flame velocity, which resulted in an increase in the height of the flame cone. To obtain the same height of the flame cone after addition of the retardants, the flow rate of the combustible mixture was reduced to achieve a flame height of 10 mm. The flow rates of combustible mixture with additions of TPPO and HBCD were about 25 and  $30 \text{ cm}^3/\text{s}$ , respectively. Since the flame front is almost identical to the freely propagating flame front, it is expected that the flow rate of the combustible mixture does not influence the flame structure. The choice of probing position relative to the flame cone was made based on visual observations of flame front and measurements of stable species profiles at different probe locations. These observations are summarized below:

- After probing near the vertex of a flame cone, stronger distortions of the flame front (inside the flame) by the probe were observed.
- Probing near the basis of the flame cone resulted in a strong aerodynamic perturbation of the flame by the probe.
- The flame region near the edge of the burner was cooled due to heat losses into the burner after addition of the flame retardant and the resultant surrounding combustion products. For this situation, it is impossible to measure concentration profiles at a distance more than 2 mm from the combustion zone because of reaction of the flame retardant additive with the surrounding air.

The optimum probe position appeared to be at a probe position 1/4 and 3/4 from the height of the flame cone based on observed concentration profiles.

Temperature distributions were measured by a 0.02-mm-diameter Pt–Pt + 10% Rh thermocouple coated with an anticatalytic protective layer of  $\text{SiO}_2$ . The total diameter of the thermocouple with the coating was 0.025–0.030 mm. For measurements in the perturbed (by the probe) flame, the thermocouple was at a distance of 0.25 mm from the tip of the probe. The heat losses of the thermocouple due to radiation were taken into account using the formula given in [13]. The accuracy of the flame temperature measure-

ments was  $\pm 30^\circ \text{C}$ . A comparison of the temperatures in the perturbed and unperturbed flames without the additive retardants showed that the introduction of the probe into the flame did not change the flame temperature within the measurement error.

Profiles of concentration of flame species were measured using MBMS with soft electron-impact ionization. The experimental setup used in the MBMS study is described in [14,15]. A quartz cone with an orifice diameter of 0.08 mm, a wall thickness of about 0.05 mm, and an internal angle at the apex of  $40^\circ$  was used as the probe. For MBMS flame studies, the burner was inclined at an angle of about  $45^\circ$  to the vertical, so that the probe axis was perpendicular to the flame front. A quadrupole mass spectrometer with an upgraded ion source using soft electron-impact ionization and small spread of electron energy was used to measure the mass spectra of the samples. The intensities of peaks at 1 (H) and 17 (OH) AMU were measured at an ionizing energy of 16.2 eV, which is low enough in energy to prevent fragmentation. The calibration coefficients for H and OH were determined by comparing their final concentrations in the postflame zone without additives. The coefficients were calculated assuming partial equilibrium of the three most rapid reactions ( $\text{H}_2 + \text{OH} = \text{H}_2\text{O} + \text{H}$ ;  $\text{H}_2 + \text{O} = \text{H} + \text{OH}$ ;  $\text{O}_2 + \text{H} = \text{OH} + \text{O}$ ) and using a method described earlier [16]. The peak intensities of stable compounds ( $\text{O}_2$ ,  $\text{CH}_4$ ,  $\text{H}_2\text{O}$ ) were measured at an ionizing energy of 18–20 eV. The calibration coefficients for these compounds were determined by direct calibrations using individual compounds and their mixtures of known composition. The relative error of peak intensity measurements for stable compounds was  $\pm 2\%$ . The measurement error associated with active species was about  $\pm 25\%$ .

The structure of the flame without retardants was simulated using PREMIX and CHEMKIN codes (SANDIA National Laboratories, USA) and the kinetic mechanism for the propane oxidation (77 species (H, O, C, N) and 469 reactions) [17,18]. This mechanism is available elsewhere [19].

### 3. Results and discussion

#### 3.1. Structure of flame

Fig. 2 gives temperature profiles in the flame without additives and doped with  $0.0190 \pm 0.001\%$  (by volume) of TPPO and with  $0.0180 \pm 0.001\%$  of HBCD. The postflame temperature of the undoped flame was 1970 K; those of HBCD-doped and TPPO-doped flames were 1860 and 1840 K, respectively. From these data one can see that addition of the flame retardants decreases the final temperature by 130 and

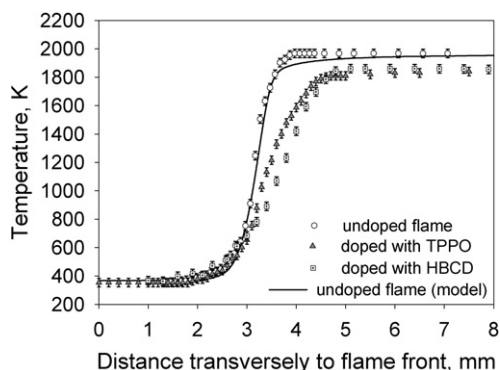


Fig. 2. Temperature profiles in  $\text{CH}_4/\text{O}_2/\text{N}_2$  flame without additive (open symbols—experiment, line—modeling) and doped with 0.019% of TPPO (triangular symbols) and 0.0180% of HBCD (square symbols).

110 K, respectively, and increases the width of the combustion zone by a factor of  $\sim 1.6$ – $1.7$ . The calculated temperature profile for the undoped flame in Fig. 2 is in good agreement with the measured profile. The decrease in the final flame temperature upon the addition of the retardants is due to several factors: (1) the thermal effect of the additive, i.e., the addition of a small amount of fuel to the rich flame; (2) an increase in the thermal perturbations of the flame by the probe due to the lower velocity of the gas flow incident on the probe; and (3) an increase in the width of the combustion zone and a decrease in the completeness of combustion of the gas mixture due to the suppression of flame reactions (the flame has a finite size, with a boundary region where fresh air supply and cooling of combustion products takes place). According to calculations, when methane is added to a combustible mixture in a small amount equivalent to the total carbon and hydrogen content in the retardant molecule, the change in the final temperature is only  $\sim 20$  K. Thus, in flames with retardants, the major contribution to the temperature-decrease effect comes from the thermal perturbations by the probe and the change in the width of the combustion zone. The larger the decrease in the flame velocity due to the addition of retardants, the larger the thermal perturbations. The observed decrease in flame temperature due to the retardants agrees qualitatively with our experimental data (given below) for the variation in flame velocity for the same type of flames.

Fig. 3 gives concentration profiles of the main stable compounds  $\text{CH}_4$ ,  $\text{O}_2$ , and  $\text{H}_2\text{O}$  in the undoped flame (experimental and modeling) and doped with TPPO and HBCD. It should be noted that for a flame stabilized on a Mache–Hebra burner, it is difficult to determine the initial point of measurement. Therefore, the initial position of the profiles in the flame was chosen arbitrarily in the region of zero concentra-

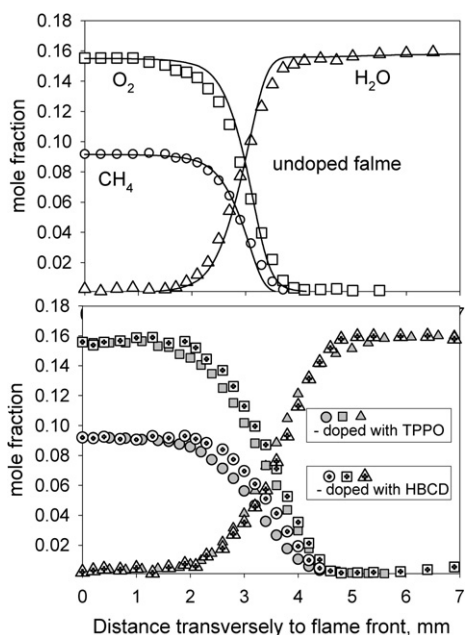


Fig. 3. Profiles of concentration of  $\text{CH}_4$ ,  $\text{O}_2$ , and  $\text{H}_2\text{O}$  in  $\text{CH}_4/\text{O}_2/\text{N}_2$  flame without additive (open symbols—experiment, line—modeling) and doped with 0.019% of TPPO (gray symbols) and 0.0180% of HBCD (cross symbols).

tion gradient. The concentration (Fig. 3) and temperature (Fig. 2) profiles clearly show that the addition of the retardants increases the width of the flame zone and slows down the chemical reactions in the flame.

In the TPPO-doped and HBCD-doped flames, phosphorus oxides and acids ( $\text{PO}$ ,  $\text{PO}_2$ ,  $\text{HOPO}$ ,  $\text{HOPO}_2$ ) and bromine-containing species ( $\text{HBr}$ ,  $\text{Br}$ ) were identified. But the concentrations of phosphorus- and bromine-containing compounds were determined with insufficient accuracy because of low retardant loading (190–180 ppm).

Fig. 4 gives H and OH concentration profiles in the flames without additives (experiment and calculation) and doped with TPPO and HBCD. From these concentration profiles, one can see that the addition of TPPO reduced both the maximum concentration of H (by a factor of 2.8) and its final concentration (by a factor of 2.6). Compared to TPPO, the addition of HBCD led to a weaker (a factor of 2) decrease in the H concentration in both the reaction and postflame zone. The addition of TPPO led to a large (a factor of  $\sim 1.7$ ) reduction in the maximum concentration of OH, but the OH final concentration decreased by only a factor of  $\sim 1.1$ . Unlike TPPO, the HBCD additive reduced both the maximum and final concentrations of OH only slightly, by a factor of  $\sim 1.1$ – $1.2$ . This suggests that the effect of flame retardants on adiabatic flames is likely related to the concentration reduction

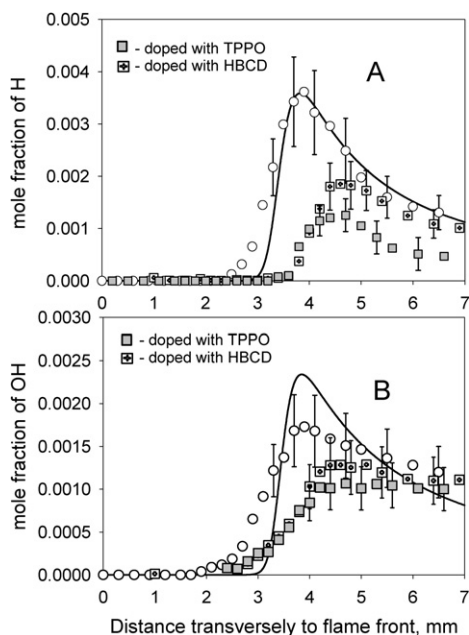


Fig. 4. Profiles of concentration of H (A) and OH (B) in  $\text{CH}_4/\text{O}_2/\text{N}_2$  flame (open symbols—experiment without additive, gray symbols—doped with 0.019% of TPPO, cross symbols—doped with 0.0180% of HBCD, line—modeling).

of active species in the reaction zone (from changes in their peak concentrations).

A comparison of the relative changes in maximum concentrations of H and OH due to the addition of the retardants leads to the conclusion that for similar retardant concentrations, TPPO suppresses the flame more effectively than HBCD because it leads to a greater reduction in the OH and H peak concentrations in the reaction zone and to a reduction in the OH concentration in the post-flame zone. It is known that the flame-retardant effect of HBCD is due to the reactions of Br with H, which should have a greater impact on the H concentration and less on the OH concentration. In the flame, TPPO as a phosphorus-containing compound is transformed to phosphorus oxides and phosphorus oxoacids [9,10], which catalyze the recombination reactions of H and OH.

In reviewing the data for this study, there is also a possibility that the reduction in concentration of H atoms and OH radicals in the flame is related to a temperature decrease (thermal factor) versus a possible radical-scavenging pathway (kinetic factor). We attempted to elucidate how the maximum (peak) concentrations of H and OH radicals change if the temperature in the postflame zone decreases by 130 K (as was observed in the flame with the retardants). Calculations show that the addition of an inert diluent ( $\sim 8\%$   $\text{N}_2$  by volume) to the combustible mixture decreases

the temperature in the postflame zone by 130 K. This will decrease the peak concentrations of H and OH by only a factor of 1.37 and a factor of 1.64, respectively. Thus, the predicted reduction in the peak concentration of H radicals due to temperature decrease is far smaller than the experimentally observed values by a factor of  $\approx 5$  and  $\approx 3$  for TPPO and HBCD, respectively. A similar situation is observed with these additives for the changes in the final H concentration in the postflame zone. In addition, based on simulation data, the reduction in the peak concentration of OH radicals for the combustible mixture diluted with  $\text{N}_2$  is close to the experimental value in the flame with TPPO. In the case of HBCD, the reduction in the peak concentration of OH radicals is smaller in the experiments than in the simulations. A similar trend (a comparable or somewhat greater effect of the thermal factor compared to the kinetic factor) is observed in the postflame zone for TPPO and HBCD. However, in this case the difference is within the experimental error ( $\pm 25\%$  rel.) for the measurement of radical concentrations in the flame.

As noted above, the largest decrease in the active species concentration is observed in the zone of chemical reactions (reduction in peak concentrations), whereas in the zone of combustion products, it is similar or much smaller. This observation suggests that the kinetic factor plays a dominant role in the reduction of the radical concentrations in the reaction zone. As was found in this study, the maximum effect of flame retardants on the active species concentration is exhibited in the zone of chemical reactions. The chemical reaction zone is the best region for quantifying overall impact of flame retardants on adiabatic flames.

### 3.2. Effect of inhibitors on burning velocity

Flame velocity was estimated by the change of flame cone height before and after addition of flame retardant. For a flame stabilized on a Mache–Hebra burner, the velocity is given by the formula  $S_u = W/s$ , where  $S_u$  is the burning velocity,  $W$  is the volumetric flow rate of the combustible mixture, and  $s$  is the area of the flame cone. Thus, the change in flame velocity due to the addition of a flame retardant can be determined by measuring the change in the height of the flame cone. In this case, the relative measurement error is about  $\pm 5\%$ . During measurement of the flame cone height, the axis of the burner was disposed vertically. This method of determining the flame-retardant effectiveness, unlike the MBMS technique, is free from the errors that can arise during probe sampling.

According to the measurements, the burning velocity of the undoped flame was  $23.5 \pm 1.1$  cm/s and

those of TPPO-doped and HBCD-doped flames were  $16.4 \pm 1.3$  and  $19.7 \pm 1.2$  cm/s, respectively. So the addition of 0.0190% (by volume) TPPO decreases the burning velocity by  $\approx 30\%$ , and the addition of 0.0180% (by volume) HBCD decreases the burning velocity by only 16%. The results of burning velocity measurements indicate that the flame-inhibition effectiveness (normalized for mole fraction) of TPPO is  $\approx 1.9$  times higher than that of HBCD. This value is in good agreement with data on the changes in the peak concentration of H radicals in the flame with retardants, where the addition of TPPO produced a  $\sim 1.8$  times larger decrease in the H concentration than HBCD. Thus, the effectiveness of TPPO is almost two times higher than HBCD.

This comparison of results obtained by two independent methods shows that MBMS is suitable for determining the relative effectiveness of retardants from changes in the peak concentration of H in flames. Flame-retardant effectiveness in this case refers to fundamental action of the flame retardant within the flame. This is a simplification, since it involves only the flame retardant and not the polymer. It also neglects the degradation pathways for both the flame retardant and the polymer. The actual effectiveness for a flame retardant in a polymer blend will depend on the degradation of the polymer with respect to the degradation of the flame retardant as well as the polymer degradation pathway. It may also depend on interactions between the flame retardant and the polymer, as well as their associated degradation species.

For all studies, the experimental concentration profiles of stable compounds, H atoms, and temperature profiles in the  $\text{CH}_4/\text{air}/\text{N}_2$  flame were in good agreement with the results from numerical simulations. This agreement confirms the usefulness of the MBMS technique for exploring combustion flame chemistry that involves chemical species. In addition, the various concentration profiles of active and stable species in the flame show the utility of the MBMS technique for studying chemical species at various zones of the flame. MBMS allows a fundamental understanding of the action of flame retardants within a flame environment which in turn is key to a fundamental understanding of flame retardant activity.

The studies described here show that the compounds tested are effective flame inhibitors. Without exerting a significant thermal effect on the flame, both flame retardants markedly decrease the flame velocity and the active species concentration in the zone of chemical reactions in the flame. Both HBCD and TPPO clearly lower the overall rate of the combustion process within the flame.

#### 4. Conclusions

1. In a freely propagating  $\text{CH}_4/\text{air}/\text{N}_2$  flame at 1 atm without and with flame retardants, the concentration profiles of stable compounds and active species (both atoms and free radicals) were measured using molecular beam mass spectrometry. The flame temperature profiles were determined with a microthermocouple technique.
2. It was found that maximum concentrations of H and OH in the flame are decreased by the addition of flame retardants HBCD and TPPO. The more effective the flame retardant on a fundamental basis, the larger the decrease in both OH and H levels.
3. Evidence was found supporting the hypothesis that the reduction in the flammability of polymer materials with the addition of flame retardants occurs by chain termination due to the chemical reactions of the retardants or their decomposition products with the chain carriers or active reaction centers, mainly H and OH.
4. It was shown that molecular beam mass spectrometry is suitable for studying the chemical structure of flames under nearly adiabatic conditions.

#### References

- [1] E.M. Pearce, Y.P. Khanna, D. Raucher, *Therm. Charact. Polym. Mater.* (1981) 793–843.
- [2] F.C.-Y. Wang, *J. Chromatogr. A* 886 (1–2) (2000) 225–235.
- [3] R. Luijk, H.A.J. Govers, G.B. Eijkel, J. Boon, *J. Anal. Appl. Pyrol.* 20 (1991) 303–319.
- [4] F. Barontini, K. Marsanich, V.J. Cozzani, *Therm. Anal. Calorim.* 78 (2004) 599–619.
- [5] J.E. Siow, N.M. Laurendeau, *Combust. Flame* 136 (1–2) (2004) 16–24.
- [6] J.W. Hastie, D.W. Bonnell, *Molecular chemistry of inhibited combustion systems*, Final NBSIR 80-2169, PB81-170375, National Bureau of Standards, 1980.
- [7] R.T. Wainner, K.L. McNessby, R.G. Daniel, A.W. Miziolek, V.I. Babushok, in: *Proceedings of Halon Option Technical Working Conference*, Center for Global Environmental Technologies, Albuquerque, NM, 2000, p. 141.
- [8] A.G. Shmakov, O.P. Korobeinichev, V.M. Shvartsberg, D.A. Knyazkov, T.A. Bolshova, I.V. Rybitskaya, *Proc. Combust. Inst.* 30 (2) (2004) 2342–2352.
- [9] O.P. Korobeinichev, V.M. Shvartsberg, A.G. Shmakov, T.A. Bolshova, T.M. Jayaweera, C.F. Melius, W.J. Pitz, C.K. Westbrook, H. Curran, *Proc. Combust. Inst.* 30 (2) (2004) 2353–2360.
- [10] T.M. Jayaweera, C.F. Melius, W.J. Pitz, C.K. Westbrook, O.P. Korobeinichev, V.M. Shvartsberg, A.G. Shmakov, T.A. Bolshova, H. Curran, *Combust. Flame* 140 (2005) 103–115.

- [11] M.A. MacDonald, F.C. Gouldin, E.M. Fisher, *Combust. Flame* 124 (4) (2001) 668–683.
- [12] H. Mache, A. Hebra, *Sitzungsber. Osterreich. Akad. Wiss. Abt. Ila* 150 (1941) 157.
- [13] W.E. Kaskan, *Proc. Combust. Inst.* 6 (1957) 134–139.
- [14] O.P. Korobeinichev, S.B. Il'in, V.M. Mokrushin, A.G. Shmakov, *Combust. Sci. Technol.* 116–117 (1996) 51–67.
- [15] O.P. Korobeinichev, V.M. Shvartsberg, A.A. Chernov, *Combust. Flame* 118 (1999) 727–732.
- [16] J. Warnatz, U. Maas, R.W. Dibble, *Combustion. Physical and Chemical Fundamentals, Modeling and Simulations, Experiments, Pollutant Formations*, Springer-Verlag, Berlin/Heidelberg/New York, 2001, chapter 7.1.2.
- [17] H.J. Curran, S.M. Gallagher, M. Conaire, J.M. Simmie, in: *Proceedings of the European Combustion Meeting 2003 (ECM-2003)*, Orleans, France, 2003.
- [18] H.J. Curran, T.M. Jayaweera, W.J. Pitz, C.K. Westbrook, *Western States Section of the Combustion Institute*, Davis, California, 2004, Paper No. 04S-58.
- [19] Available at: [http://www.kinetics.nsc.ru/labor/kcp\\_en/opc\\_mech.html](http://www.kinetics.nsc.ru/labor/kcp_en/opc_mech.html).